

Phenoxy resin-based vinylogous urethane covalent adaptable networks

Original

Phenoxy resin-based vinylogous urethane covalent adaptable networks / Soavi, G., Portone, F., Battegazzore, D., Paravidino, C., Arrigo, R., Pedrini, A., Pinalli, R., Fina, A., Dalcanale, E.. - In: REACTIVE & FUNCTIONAL POLYMERS. - ISSN 1381-5148. - STAMPA. - 191:(2023). [10.1016/j.reactfunctpolym.2023.105681]

Availability:

This version is available at: 11583/2985101 since: 2024-01-15T22:32:27Z

Publisher:

ELSEVIER

Published

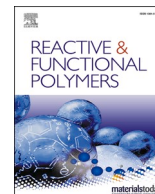
DOI:10.1016/j.reactfunctpolym.2023.105681

Terms of use:

This article is made available under terms and conditions as specified in the corresponding bibliographic description in the repository

Publisher copyright

(Article begins on next page)



Phenoxy resin-based vinylogous urethane covalent adaptable networks

Giuseppe Soavi^a, Francesca Portone^a, Daniele Battegazzore^b, Chiara Paravidino^b,
Rossella Arrigo^b, Alessandro Pedrini^a, Roberta Pinalli^a, Alberto Fina^{b,*}, Enrico Dalcanale^{a,*}

^a Department of Chemistry, Life Sciences and Environmental Sustainability and INSTM UdR Parma, University of Parma, Parco Area delle Scienze 17/A, 43124 Parma, Italy

^b Dipartimento di Scienza Applicata e Tecnologia, Politecnico di Torino, Viale Teresa Michel 5, 15121 Alessandria, Italy

ARTICLE INFO

Keywords:

Vitrimer
Vinylogous urethane
Phenoxy resin
Covalent adaptable networks

ABSTRACT

This work presents a post-polymerization approach to the preparation of vitrimers, exploiting the transamination of vinylogous urethane in linear phenoxy resins. Phenoxy vitrimers are obtained by a two-steps synthesis from a commercial phenoxy resin via partial conversion of hydroxyl groups to acetoacetates (AcAc), followed by network formation by reaction with *m*-xylylendiamine as crosslinker. Three different vitrimers with variable crosslinking density are obtained by tuning the density of AcAc moieties along the phenoxy resin scaffold (5%, 10% and 15% conversion of hydroxyl groups). The conversion of linear polymers to dynamic crosslinked networks is confirmed by dynamic mechanical thermal analyzer and rheology measurements, followed by stress relaxation tests to investigate the kinetics of bond exchanges. Tensile tests as a function of reprocessing cycles reveal an increase of the maximum elongation and stress at break and prove the good recyclability of the vitrimers. Enhanced adhesive properties compared to pristine phenoxy resins are demonstrated, including the possibility to thermally re-join the assembly after its mechanical failure. Finally, the solvent-free preparation of vitrimers is explored at 5% crosslinking density via melt reactive blending, providing a valuable alternative to the less environmentally sustainable synthesis in solution.

1. Introduction

Epoxy resins are widely used in several large-scale applications, including electronics, structural composites and adhesives. Standard epoxy resins are thermosets, therefore unsuitable to be repaired and recycled. However, their non-recyclability poses environmental problems, whose solution asks for sustainable alternative materials, as required by the EC Circular Economy Action Plan [1]. In the last few years, this drawback has been addressed in an innovative way, by introducing epoxy vitrimers [2]. Vitrimers bridge the gap between thermoplastics and thermosets, having the mechanical properties of the latter at service temperature and malleability like glass at temperature above the topology transition temperature (T_v) [3]. This bimodal behavior is obtained by introducing covalent adaptable networks (CANs) in the polymer in the form of thermally activated reversible covalent bonds.

The cross-link density in vitrimers is constant, due to bond cleavage occurring only after formation of new bonds [2]. Consequently, the viscosity in the melt is controlled by the exchange reactions, following

an Arrhenius-like decrease with temperature akin to vitreous silica [2], providing glass-like weldability [4]. Pioneered by Leibler and co-workers, the earliest examples of epoxy vitrimers were based on dynamic transesterification reactions, catalyzed by zinc acetate [2,3]. Subsequently, other different exchange chemistries have been explored for the preparation of epoxy vitrimers such as disulfide metathesis [5], imine amine exchange [6,7], vinylogous urethane [8] and silyl ether exchange [9]. All these epoxy vitrimers are prepared by reacting the epoxy resins with a suitable hardener, either forming or containing the exchangeable bond. Absent in this scenario is the post-polymerization approach, where an epoxy-based linear thermoplastic is converted into a vitrimer.

Phenoxy resins are commercially available amorphous thermoplastic polymers with molecular weight in the range 10,000–100,000 g/mol. They are miscible with epoxy resins, with whom they are often blended. Due to their excellent mechanical properties including flexibility, toughness, adhesive and cohesive strength, as well as chemical and heat resistance, phenoxy resins are widely employed in composites and adhesives. Phenoxy resin vitrimers are unknown in the literature. The

* Corresponding authors.

E-mail addresses: alberto.fina@polito.it (A. Fina), enrico.dalcanale@unipr.it (E. Dalcanale).

<https://doi.org/10.1016/j.reactfunctpolym.2023.105681>

Received 26 May 2023; Received in revised form 26 July 2023; Accepted 28 July 2023

Available online 30 July 2023

1381-5148/© 2023 The Authors. Published by Elsevier B.V. This is an open access article under the CC BY-NC-ND license (<http://creativecommons.org/licenses/by-nc-nd/4.0/>).

pendant hydroxyl groups in phenoxy resins are amenable to a variety of functionalization. Among the several CAN chemistries available, we selected vinylous transamination [10] to turn phenoxy resins into vitrimers (Scheme 1). The main advantage related to the use of vinylous urethane group is the increased electrophilicity of vinylous urethane bond, in contrast to conventional urethane bonds. Indeed, the conjugated C=C can act as Michael acceptor in the nucleophilic addition of an amine group without the need of catalysts [10]. This higher reactivity leads to the vitrimeric properties of the corresponding polymers above the T_v . For this aim, commercial phenoxy resins were partially derivatized with acetoacetate (AcAc) groups and the resulting polymers were crosslinked with *m*-xylylendiamine (XYDIA). Mechanical and viscoelastic properties were thoroughly investigated, to exploit the vitrimeric properties in reprocessability and toward the development of reversible adhesives. Finally, the solvent-free preparation of phenoxy vitrimers via melt reactive blending was explored.

2. Experimental

2.1. Materials and methods

2.1.1. Synthesis

Unless otherwise specified, chemicals and solvents were purchased from Sigma-Aldrich and used as received. Linear phenoxy resin was purchased from Gabriel Chemistry (US), grade PKHB, avg. molecular weight 32 kDa, 277 g/equiv. OH. In the following, the pristine phenoxy polymer is referred to as PKHB. PKHB grafted with acetoacetate are referred to as PKHB n% AcAc, while vitrimers obtained are referred to as PKHB n% VU.

2.1.1.1. General procedure for the synthesis of PKHB 5,10,15% AcAc. 10 g of PKHB (35.17 mmol) were dissolved in 50 mL of methyl ethyl ketone (MEK) at 25 °C. After heating to 82 °C, 1.16 mL (5%), 2.31 mL (10%), 4.05 mL (15%) respectively of tert-butoxy acetoacetate (corresponding to 7.03, 14.06 and 24.61 mmol) were added under magnetic stirring. After 5 h in refluxing MEK, 400 mL of methanol were added to the solution. The resulting white precipitate was filtered and dried in vacuum oven at 10^{-2} Torr and 60 °C for 24 h and then characterized via ^1H NMR (Fig. S1) and FTIR-ATR (Fig. 1).

2.1.1.2. General procedure for the synthesis of PKHB 5,10,15% VU. 8 g of PKHB 5,10,15% AcAc corresponding to ≈ 27 mmol of each polymer, were dissolved in 40 mL of MEK, then *m*-xylylendiamine (XYDIA) diluted in 1 mL of MEK was added to the solution in a 0.6 molar ratio with respect to the molar amount of AcAc groups present on PKHB (0.11

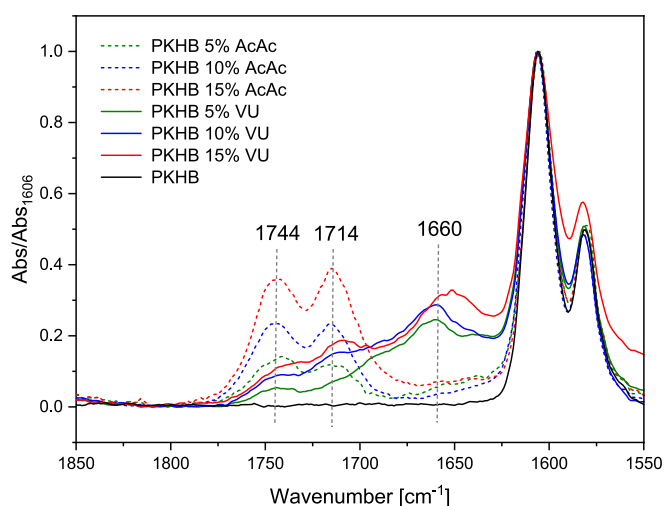
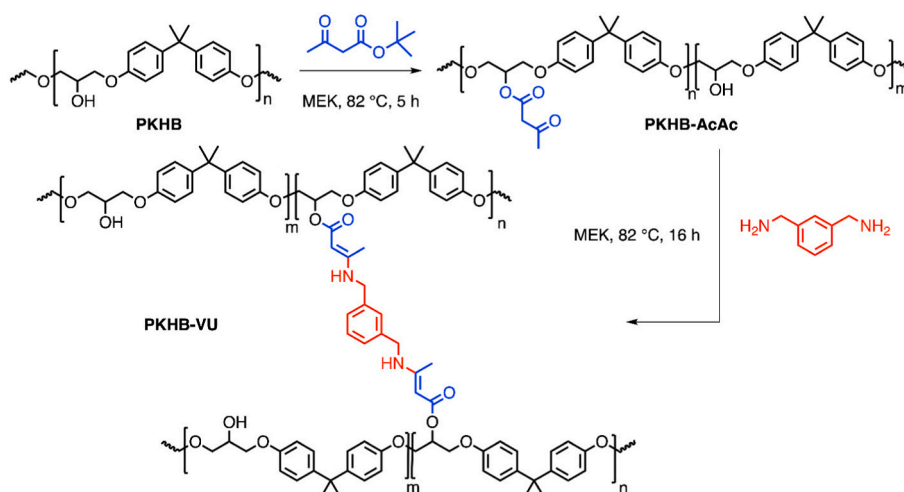


Fig. 1. Spectral window of FTIR of PKHB (solid black line), PKHB n% AcAc (dashed lines) and PKHB n% VU (solid colored lines), evidencing the diagnostic absorption bands relative to the carbonyl stretching.

mL for 5%, 0.22 mL for 10% and 0.32 mL for 15%, details reported in Table S1). After stirring for 16 h in refluxing MEK, a yellow precipitate was formed. The resulting suspension was treated with 300 mL of methanol, and the resulting precipitate was filtered and dried in vacuum oven at 10^{-2} Torr and 60 °C for 24 h.

2.1.1.3. Preparation of PKHB 5% VU in melt reactive blending. Solvent-less synthesis was implemented into a co-rotating twin-screw mini-extruder DSM Xplore 15 cm³ under nitrogen flow, at 240 °C, 100 rpm, 10 min. 10.0 g of PKHB-AcAc 5% (1.73 mmol eq. AcAc) were pre-wet with 0.137 mL of xylene diamine (1.04 mmol corresponding to a molar ratio AcAc/XYDIA = 0.6), loaded in the chamber at 50 rpm, then increased to 100 rpm for the mixing stage (10 min) and the final extrusion. Vitrimer prepared by melt reactive blending is referred to as PKHB-VU 5%_MELT.

2.1.1.4. Gel fraction determination. Gel fractions were calculated based on dry residual weight after dissolution in methyl ethyl ketone (MEK) for 24 h. Specimen's pieces were placed in a 10 mL closed vial and heated in MEK at 60 °C for 24 h. After Büchner filtration, the samples were dried in vacuum oven at 10^{-2} Torr and 100 °C for 24 h. The gel fraction was determined according to the equation below:



Scheme 1. Synthetic scheme for the preparation of PKHB n% AcAc and PKHB n% VU compounds ($n = 5, 10, 15$).

$$\text{Gel fraction (\%)} = \frac{m_{\text{final}}}{m_{\text{initial}}} \cdot 100.$$

2.1.2. Characterization

2.1.2.1. Nuclear magnetic resonance (NMR). NMR spectra were recorded on a Bruker Avance 400 (400 MHz) in chloroform (CDCl_3) at 25 °C. ^1H NMR chemical shifts are given in reference to the residual solvent peak of CDCl_3 at 7.26 ppm.

2.1.2.2. Infrared spectroscopy (IR). Attenuated Total Reflectance Fourier Transformed Infrared spectra (FTIR-ATR) were acquired on a Perkin Elmer FT-IR Spectrum Two, equipped with a diamond crystal. The frequency range from 4000 cm^{-1} to 400 cm^{-1} for 32 scans and with 4 cm^{-1} resolution was used. Absorbance spectra were baseline-subtracted and normalized to the intensity at 1606 cm^{-1} , corresponding to aromatic C=C stretching, taken as a control peak.

2.1.2.3. Dynamic mechanical thermal analyses (DMTA). DMTA analyses were carried out on bars with a cross-section of around 6 × 1 mm², 30 mm length, cut from compression-molded plates, tested in tensile mode on a Q800 equipment (TA Instruments). Temperature scan was from room temperature to 170 °C, at 2 °C/min heating rate and 1 Hz frequency in strain-controlled mode, deformation amplitude at 0.05% and 0.01 N preload. Minimum stress allowed (additional end-of test criterion) was set at 0.1 MPa, except for pristine PKHB, in which 1 MPa was used to prevent possible dripping. All samples were conditioned at 23 °C and 50% of relative humidity for at least 48 h before analyses.

2.1.2.4. Rheology. Rheological properties were investigated using an ARES rheometer (TA Instruments) operated with a 25 mm parallel plate geometry and 1 mm thickness samples. Dynamic frequency sweep tests were carried out to determine G' , G'' and complex viscosity (η^*) between 0.1 and 100 rad/s at 1% strain (linear viscoelasticity) at a constant temperature of 200 °C. Isothermal relaxation tests were also carried out at 5% strain, till below 30% of the initial stress was reached. Stress $G(t)$ is reported normalized on G_0 , i.e. the stress recorded at $t = 1$ s to get rid of instrumental transient at the start for relaxation test [11].

2.1.2.5. Mechanical properties. Tensile tests were done on 60 × 10 mm² compression molded films, thickness in the range of 150 to 200 μm , on an Instron 5966 machine equipped with a 50 N loading cell and flat faces pneumatic clamps, gauge length of 30 mm. Strain rate was 1 mm/min up to 0.3% strain and then 2 mm/min to break. The samples were conditioned at 23 °C and 50% of relative humidity for at least 48 h before analyses. Tests carried out on films prepared from as-obtained vitrimers are referred to as cycle 1. After testing, broken specimens were recovered and reprocessed by compression molding into new films in the same conditions and tested again, with results referred to as cycle 2. Further reprocessing with the same procedure provided tensile results referred to as cycle 3. For each composition/cycle a minimum of 4 specimens were tested. Averaged results are reported with their experimental deviations.

2.1.2.6. Adhesion tests. Single lap shear adhesion tests were carried out on the same machine, on samples prepared according to ISO 4587, using 1.5 mm thick aluminum plates pre-cleaned with ethanol. Films of 200 μm were placed between Al plates, preheated for 3 min and hot pressed under 1 ton for 5 min at 240 °C for vitrimers and 170 °C for pristine PKHB, using a lab made support to hold metal plates in proper position during compression. Tests carried out on the obtained joints are referred to as cycle 1. After joint failure, the two parts were recovered and recompressed in the same conditions and tested again, with results referred to as cycle 2. 3 specimens were tested for each composition/cycle. Averaged results are reported with their experimental deviations.

3. Results and discussion

3.1. Preparation of vitrimers

PKHB-based vitrimers were prepared in solution in two steps. Partial functionalization of PKHB with acetoacetate (AcAc) groups was carried out using t-butoxy acetoacetate in refluxing MEK (Scheme 1). The degree of functionalization was determined via ^1H NMR (Fig. S1), by integrating the diagnostic triplet of the methyne α to AcAc at 5.54 ppm against the triplet of the methyne bearing the unreacted PKHB hydroxyl groups at 4.37 ppm. Functionalized PKHB-AcAc were then reacted with XYDIA (20% excess) in refluxing MEK, to produce vinylogous urethane exchangeable crosslinking between linear chains.

Conversion to vinylogous urethane was monitored by FTIR. Infrared spectra (Fig. 1) for PKHB n% AcAc evidences the appearance of two signals at ca. 1744 and 1714 cm^{-1} , corresponding to the C=O stretching modes in the ester and ketone, respectively, with intensities proportional to the % of grafted AcAc groups. After reaction with XYDIA (Scheme 1), conversion to vinylogous urethane is supported by the appearance of a new broad band at ca. 1660 cm^{-1} , assigned to the conjugated C=O ester stretching in vinylogous urethane [12], and the disappearance of the 1744 and 1714 cm^{-1} AcAc bands. The second characteristic band of VU, namely the C=C stretching, is overlapping to the PKHB and XYDIA aromatic C=C stretching at 1606 cm^{-1} (Fig. 1).

To verify the crosslinked character and improved solvent resistance of PKHB-VU n%, the samples were kept in MEK at 60 °C for 24 h. The remaining insoluble fractions after solvent removal and vacuum oven drying were 78, 97 and 100% for 5, 10 and 15% VU, respectively. By comparison, pristine PKHB resulted completely soluble in MEK at room temperature. Such high residues in the 10 and 15% samples reflect high crosslinking degrees in PKHB-based vitrimers, in line with previously reported polyvinylogous urethanes [10]. Thermoxidative stability of the vitrimers was assessed by TGA (Fig. S2) which demonstrated no significant network decomposition until 330 °C.

Reprocessability of PKHB n% VU was tested by compression molding, allowing simple preparation of films and slabs under mild conditions, thus evidencing the dynamic nature of the crosslinking bonds. Gel fractions were re-evaluated after compression molding into sheets, to evaluate the evolution of crosslinking upon reprocessing. The residue after extraction of the soluble fraction increased to 90% for PKHB 5% VU, whereas residual fractions for 10 and 15% PKHB-VU remained constant, as the crosslinking obtained from the synthesis was quantitative, within experimental errors of the gel fraction method. Viscoelasticity of PKHB vitrimers was investigated by DMTA on heating (Fig. 2). Pristine PKHB exhibits a room temperature storage modulus E' at about 1.75 GPa, quickly decaying above 70 °C due to the α relaxation of linear chains, with a maximum temperature (T_{α}) of ca. 93 °C (Fig. 2 top). Vitrimers resulted in slightly higher storage modulus (ranging between 2.1 and 2.9 GPa) and variable T_{α} (Fig. 2 bottom) with a broad transition suggesting coexistence of relatively long linear fractions together with regions with high crosslinking densities. However, the most relevant result from the DMTA analysis is the higher thermomechanical resistance of vitrimers compared to the pristine PKHB, at temperatures well above α relaxation. Indeed, at 5% VU, the storage modulus is slowly decreasing with increasing temperature, reflecting a partial crosslinking, whereas at higher % VU clear rubbery plateaus are observed at 1.9 and 3.0 MPa for 10% and 15% VU, respectively, in agreement with calculated gel fractions.

To further investigate the viscoelastic properties at high temperature, rheological analysis was carried out at variable frequency and different temperatures in the linear viscoelastic regime. In Fig. 3, storage modulus (G'), loss modulus (G'') and complex viscosity (η^*) plots obtained at 200 °C are plotted vs. the oscillation frequency. Remarkable G' values, in the range 10⁴ to 10⁵ Pa, were obtained for the vitrimers: in 5% VU a weak dependence on frequency is observed, whereas for 10 and 15% VU frequency-independent plateau values are obtained, increasing

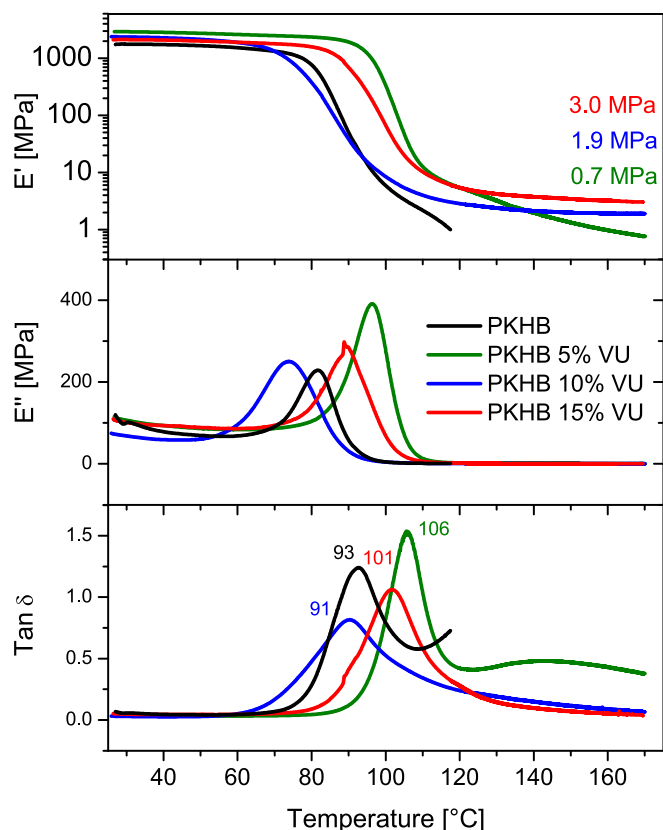


Fig. 2. DMTA plots for pristine PKHB and PKHB $n\%$ VU ($n = 5, 10, 15$). Temperature for the maximum of $\tan \delta$ plots are marked for each plot.

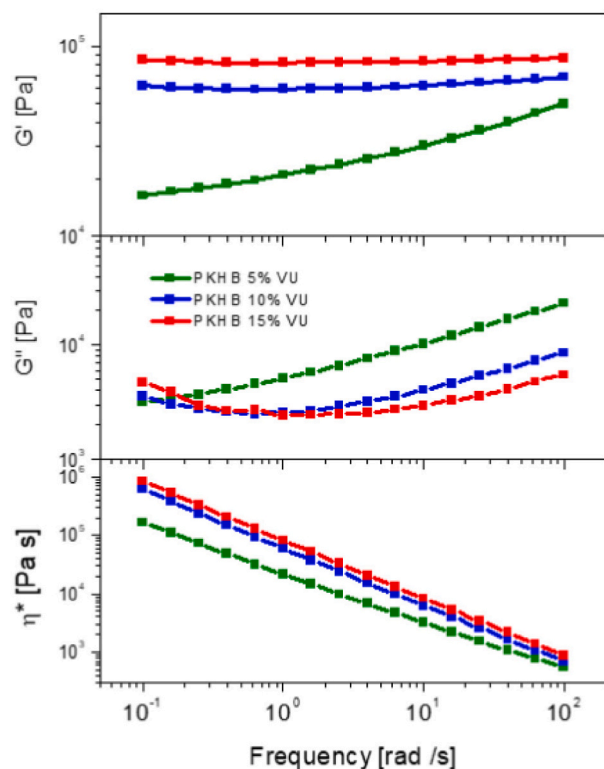


Fig. 3. Rheological plots for PKHB $n\%$ VU ($n = 5, 10, 15$).

with the concentration of crosslinking. This behavior, being completely different to that of linear PKHB and PKHB-AcAc (Fig. S3), corresponds to conversion of linear polymers to highly crosslinked networks, characterized by a solid-like rheological behavior. This is further supported by the analysis of G'' values, being significantly lower than G' for all vitrimers, and the η^* plots evidencing for extremely high viscosity up to ca. 10^6 Pa·s at low frequency, with a strong shear thinning effect as the frequency increases.

Such a viscoelastic behavior is clearly due to the covalent crosslinking of vitrimers while the exchange of bonds is not significant under these testing conditions, characterized by low deformation and limited relaxation time for the given temperature. To investigate the dynamics of bond exchanges in the covalent adaptable network, stress relaxation tests were also carried out. In these conditions, the rearrangement of the network is possible and a characteristic relaxation time as well as the activation energy can be estimated. The simplest model applicable to the stress relaxation of vitrimers assumes a simple exponential decay according to Maxwell model, with a characteristic decay time τ corresponding to the time at which the normalized stress reaches $1/e$ threshold. This model was applied to different vitrimers with high crosslinking density, including vinylous urethanes [13]. However, at low crosslinking density, deviations from the Maxwell model were reported [11] and explained by the contribution of additional relaxation modes other than the exchange reaction in CAN. These modes may include networks strands, dangling chains and trapped loops [14] as well as direct associative interaction between linear chains, including hydrogen bonding, π - π interaction and Van der Waals forces. While these additional relaxation modes may be better described in terms of a continuous relaxation spectrum [15], a simpler approach was also proposed by the use of modified decay functions [11], aiming at the estimation of an average relaxation time. Alternatively, relaxation times in vitrimers were calculated from the initial slope of the stress relaxation curve [16] or from the G' - G'' crossover frequency [15]. Regardless the method to calculate the relaxation time, the temperature dependence of relaxation times may provide information on the exchange of dynamic bonds, as vitrimers follow an Arrhenius dependency.

Stress relaxation plots for PKHB vitrimers (Fig. 4a-c) exhibit very different feature depending on the % of crosslinkers. For samples PKHB 10 and 15% VU, stress relaxation qualitatively follows the usual trend for vitrimers, with slow stress decay vs time, whereas for sample PKHB 5% VU the decay is much faster in the early stage of the test, confirming the limited crosslinking. Fitting of these relaxation plots with the Maxwell model (Fig. S4 left) did not provide good match for any of the PKHB vitrimers. However, a much better fit (Fig. S4 right) for the same was obtained with a “stretched” exponential decay function $\frac{G(t)}{G_0} = Ae^{-\left(\frac{t}{\tau}\right)^\alpha}$, with typical α values between 0.4 and 0.6 for PKHB 10 and 15% VU, in agreement with previously reported stress relaxation of vinylous urethane crosslinked polyethylene [11]. The observed deviation from the Maxwell relaxation is explained by the additional relaxation modes (e.g. networks strands, dangling chains, trapped loops as well as associative interaction between linear chains) beside vinylous urethane bond exchange. The contribution of the additional relaxation modes is more evident at low crosslinking density (5% VU), resulting in low α values (Fig. S4 right), whereas the deviation from the ideal relaxation model becomes less important at higher % VU. Representing the multi-mode relaxation with a single averaged relaxation time appears a reasonable approximation to discuss the evolution of relaxation time with temperature and to calculate the energy of activation for the relaxation process. Results reported in Fig. 4d confirm the Arrhenius type temperature dependence of the relaxation time, with best $\ln(\tau)$ vs. $1/T$ linear fit obtained for PKHB 15% VU, whereas limited scatter observed at lower crosslinking density may reflect the complexity of relaxation discussed above. Expectedly, activation energies for the relaxation process are also dependent on the VU %. At 5% VU the calculated energy of activation is as low as 69 kJ/mol, reflecting a

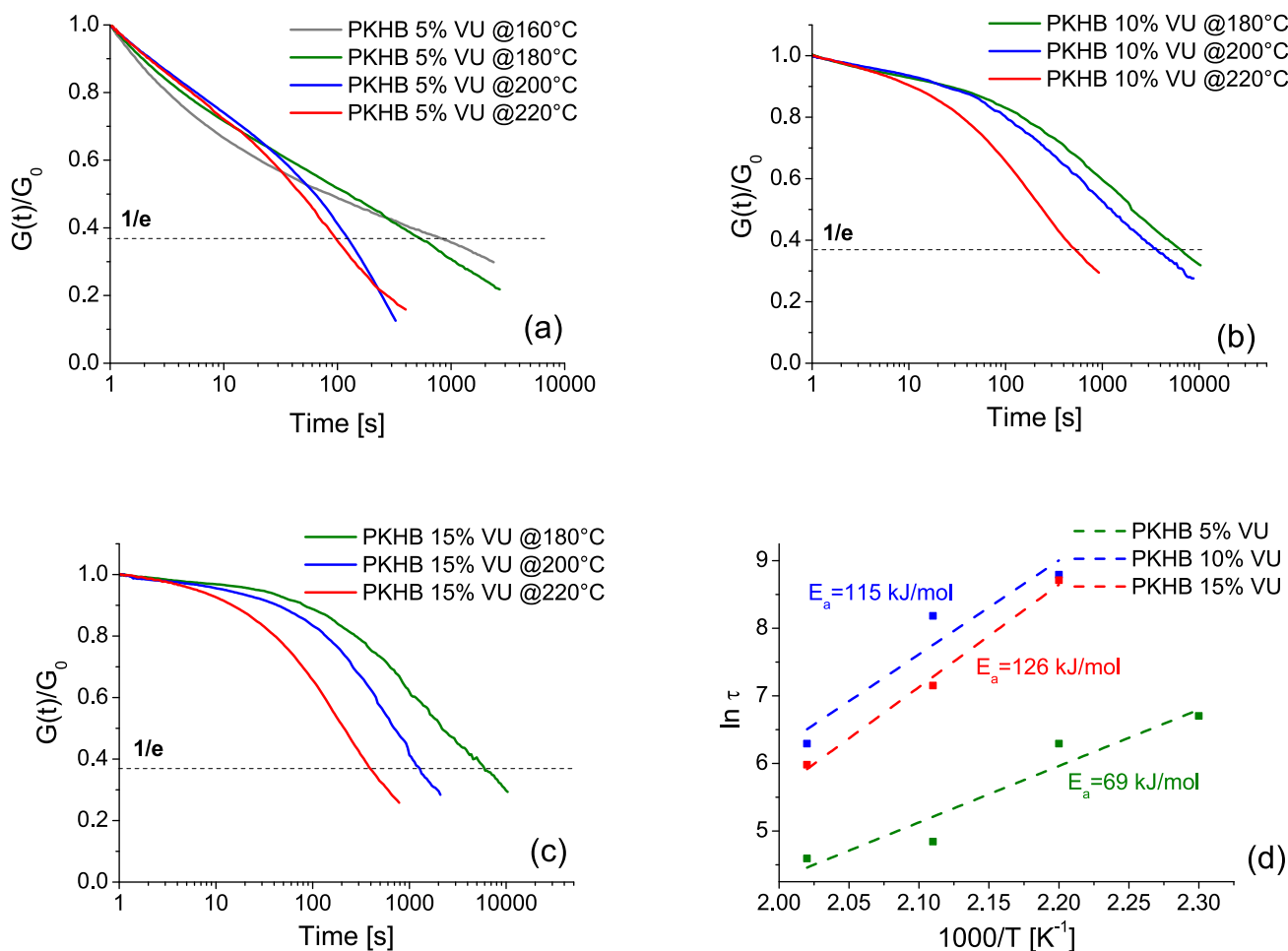


Fig. 4. Normalized stress relaxation plots at different isotherms for PKHB 5% VU (a), PKHB 10% VU (b), and PKHB 15% VU (c). Panel (d) reports Arrhenius plots for the relaxation times (τ) and fitting to calculate activation energies for the relaxation process.

significant contribution of non-crosslinked chains to the materials relaxation. The activation energy increases with cross-linking density, namely 115 and 126 kJ/mol at 10% and 15% VU, respectively. These values are higher than the ones reported for polyvinylous urethane [10] and VU crosslinked polyethylene [11] owing to the higher conformational stiffness of the aromatic structure of the phenoxy resin. Nevertheless, similar values are reported in the literature for other vitrimeric systems [17–19] and these values do not hamper the flow of the vitrimers during reprocessing at moderate temperatures [20].

The topology-freezing transition temperature (T_v) was defined by Leibler et al. [13] as the temperature at which “the mechanical relaxation time controlled by the exchange reaction rate becomes longer than the experimental timescale and, on this timescale, the network topology is frozen”. Assuming a liquid-solid transition at $\eta = 1 \cdot 10^{12}$ Pa·s and relaxation according to Maxwell’s equation $\eta = (E'/2(1 + \nu)) \cdot \tau$, where E' is the elastic modulus at the rubbery plateau and ν is the Poisson’s ratio, T_v values are easily estimated. This simple model was largely applied in vitrimers literature and results correlated with the possibility to reprocess the vitrimers at temperatures above T_v . As the bond exchange within a vitrimer network requires sufficient chain mobility, topology freezing transition is expected to occur above the glass transition temperature (T_g), as originally proposed by Leibler et al. However, T_v values below T_g were also reported in literature [10,21], yielding materials in which stress relaxation is controlled by the segmental motion of linear chains. It is worth mentioning that the above discussed assumptions for the calculation of T_v might not be accurate for vitrimers exhibiting a rheological complex behavior. In particular, when the

vitrimer relaxation is based on both bond exchanges and additional relaxation modes (e.g., networks strands, dangling chains, trapped loops etc.) Maxwell’s equation may not be a good approximation and its application may lead to misleading T_v values. In this work, since at low crosslinking degree the co-existence of different relaxation modes is apparent based on the above stress-relaxation plots (Fig. 4a), calculation of T_v for PKHB 5% VU is not possible by the Maxwell model. Instead, in highly crosslinked PKHB-VU vitrimers, the contribution to any additional relaxation mode appears negligible compared to the relaxation by vinylous bond exchanges and the Maxwell equation can be applied, resulting a T_v of 120 °C for PKHB 15% VU, which is slightly higher than the glass transition temperature for linear PKHB.

The tensile properties and recyclability of the synthesized vitrimers were evaluated. Both pristine PKHB and derived vitrimers exhibited brittle fracture (Fig. S5), regardless of the processing cycles, as expected by the relatively high glass transition temperature. Stress-strain plots (Fig. 5a for cycle 1 and Fig. S6 for cycles 2 and 3) show significant differences between vitrimers and PKHB. Elastic modulus, elongation at break and resistance at break values for the different formulations and processing cycles are reported in Table S2 and resumed in Fig. 5b, c and d, respectively.

Elastic modulus of PKHB was measured in the range of 1.6 GPa, with variations upon reprocessing cycles within the experimental error. On cycle 1, significantly higher stiffness was observed for the vitrimers, up to 3.2 GPa for PKHB-VU 10%. However, this stiffening effect is not retained on subsequent processing cycles, in which the different vitrimers appear to level off in stiffness at the value for PKHB, within the

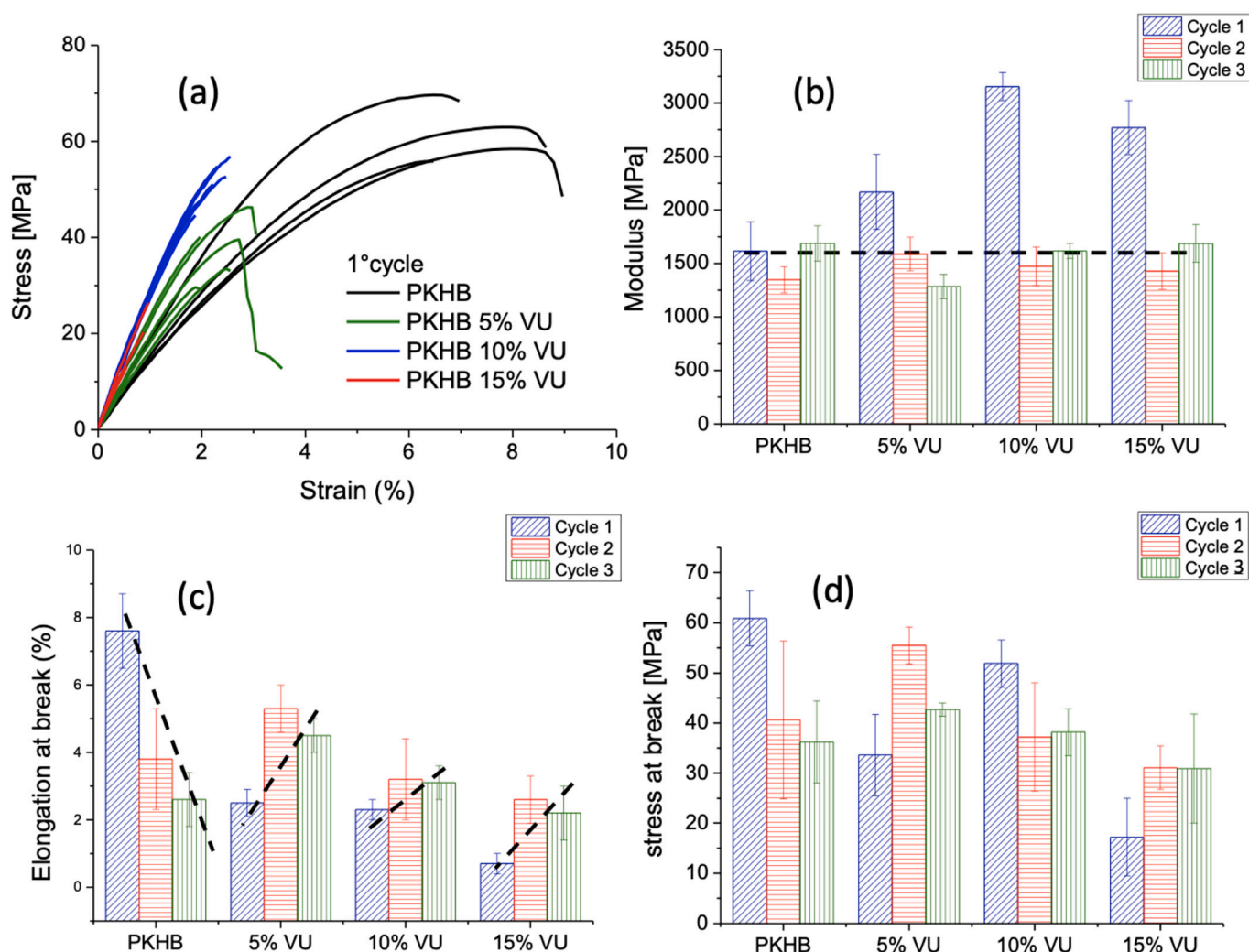


Fig. 5. Stress-strain plots on first tensile test cycle (a) and comparative histograms for different formulation and processing cycles, regarding elastic modulus (b), elongation at break (c) and stress at break (d).

experimental uncertainty. For PKHB, both elongation at break and stiffness decrease upon reprocessing cycles, according to the progressive thermo-mechanical degradation of the polymer. On the other hand, vitrimers exhibit a different trend, with typically higher elongation and resistance after reprocessing. Indeed, in CANs the polymer degradation by chain scission is still possible but the effect is not significant as the crosslinking between linear PKHB chains does not lead to a decrease in the average molecular weight, which is typically associated with embrittlement.

Adhesive properties of vitrimers were also explored and compared to pristine PKHB in lap shear test using aluminum plates. PKHB exhibits moderate adhesive properties, quantified as $3.7 \pm 0.6\%$ strain and 2.5 ± 0.4 MPa stress at failure, which occurs by cohesive-adhesive mixed mode fracture, with traces of adhesive on both surfaces of the substrate. PKHB-VU vitrimers displayed enhanced properties compared to PKHB (Fig. 6a); in particular, in PKHB 5% VU ultimate strain and stress increase to $6.5 \pm 0.8\%$ and 4.8 ± 0.5 MPa respectively. Further increase in crosslink density did not provide further enhancement but rather a decrease in joints performance, with failure by a clear adhesive mechanism (Fig. 6b). This may be related to the differences in conformational mobility of the vitrimers during the joining process and suggest slow relaxation of the highly crosslinked vitrimers, requiring higher time/temperature to optimize adhesion onto the substrate. Instead, the co-existence of different relaxation modes observed at weakly crosslinked PKHB 5%VU appears to couple good substrate adhesion with

mechanical resistance, which demonstrates potential for the development of vitrimeric adhesives. Indeed, this class of adhesive allows multiple debonding and re-bonding, based on the retained mechanical properties upon reprocessing demonstrated above. The possibility to re-join the two parts after the lap shear test was explored by simple restacking and pressing in the same conditions as for the initial bonding. While re-joining was not successful with pristine PKHB, all vitrimers joints were qualitatively satisfactory and were tested again in lap shear. Results demonstrated enhancement both in lap shear strength and in strain at break, that are, for all vitrimers, higher compared to the first cycle. For instance, PKHB 5%VU on test #2 showed $9.9 \pm 1.2\%$ strain (+52% compared to PKHB) and 5.6 ± 0.5 MPa (+16% compared to PKHB), thus demonstrating the adhesive reversibility (Fig. 6c,d and Table S3).

To avoid the use of organic solvents in vitrimers preparation, which is not appealing for industrial processes, the solvent-free preparation of phenoxy vitrimers was explored. Compared to vitrimers based on conventional thermoplastic polymers in which melt reactive blending preparation was previously reported, such as polyethylene [11], PMMA and PS [23], melt processing of phenoxy resin is significantly more challenging, owing to its relatively high glass transition temperature coupled with adhesive properties onto the metal surfaces in melt mixers. With the aim of exploring feasibility of melt processing of phenoxy VU vitrimers, and based on the physical properties discussed above, PKHB 5% VU was selected for preparation via melt reactive blending.

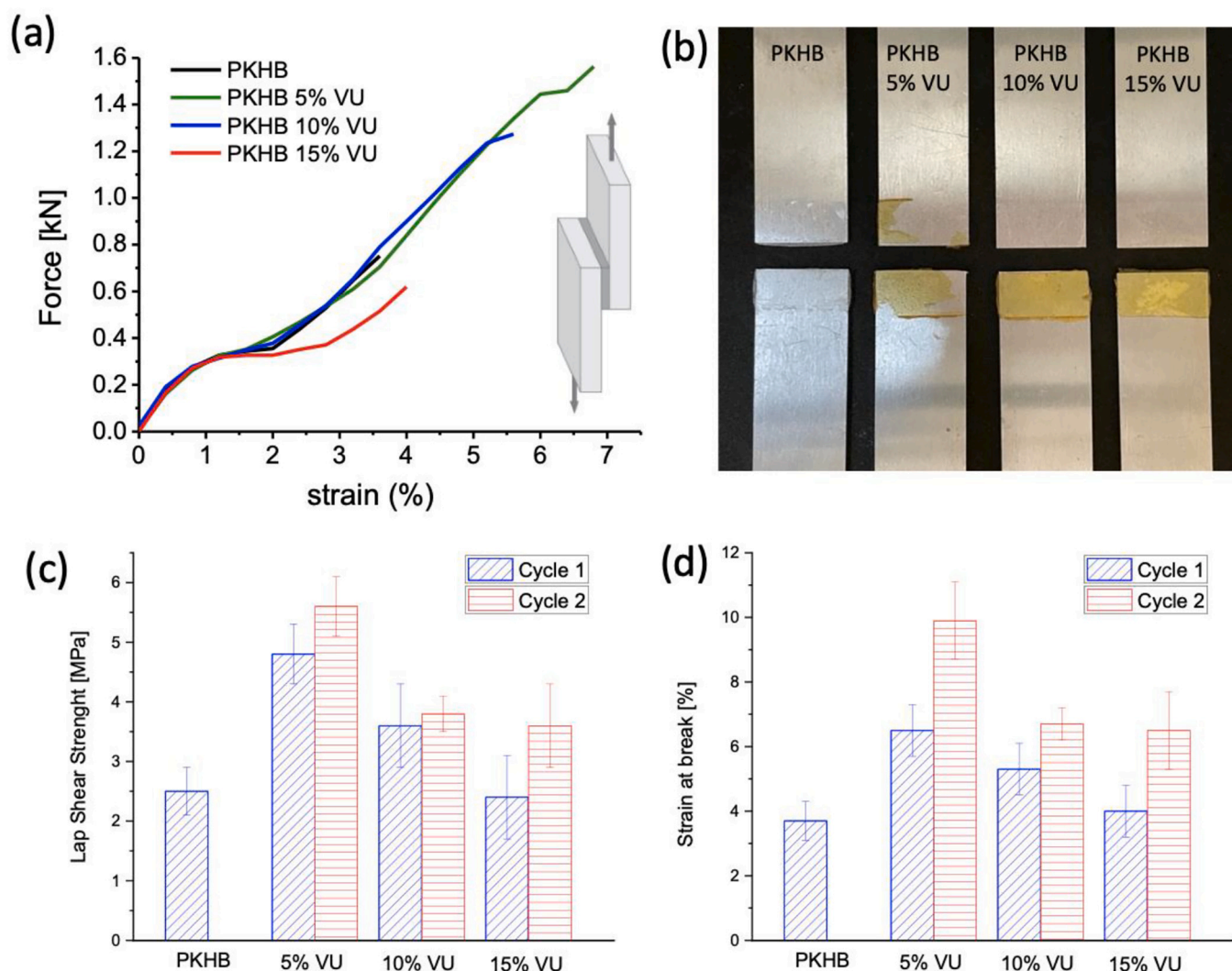


Fig. 6. Force vs strain plots for lap shear test using PKHB or vitrimers as adhesive (a) and pictures of the two plates after joint failure, for each of the adhesives (b). Panels (c) and (d) resume lap shear strength and strain at break for the different adhesives, on first and second joining cycle.

Occurrence of crosslinking during melt mixing in the presence of XYDIA is evidenced by a strong increase in melt viscosity during mixing (Fig. S7), almost up to the limit of the micro compounding system used. The gel fraction of the extruded materials was 89%, which is higher than the corresponding formulation prepared in solvent, confirming the efficiency of melt reactive blending to promote chemical reaction, thank to both high temperature and shear deformation in the melt. PKHB 5% VU_MELT was also compression molded to obtain suitable specimens for DMTA (Fig. 7a) and rheological analysis (Fig. 7b), which were found fully consistent with the reference formulation via the solvent process. Thus, the melt reactive blending can be considered a viable route to obtain phenoxy vitrimers.

4. Conclusions

Linear phenoxy resins were functionalized with acetoacetate groups to introduce reactive moieties for subsequent reaction with a diamine to produce vinylogous urethane exchangeable bonds. This allowed preparing covalent adaptable networks based on a linear equivalent of conventional epoxy, providing epoxy vitrimers, which have been validated for melt processability and recycling. The novel approach demonstrated in this work allows tailoring the crosslinking density, by varying the density of AcAc moieties along the phenoxy resin, yielding tailorable rheological properties.

Indeed, full crosslinking of the polymer was obtained at relatively high density of functional groups (e.g. 15% conversion of hydroxyl groups along the phenoxy chains), whereas incomplete crosslinking was observed at low density (e.g. 5% conversion of hydroxyl groups), yielding a rheological behavior intermediate between typical vitrimers and thermoplastic polymers. This is evidenced by the elastic and viscous moduli as a function of deformation frequency at high temperature, as well as the stress relaxation results, suggesting the combination of secondary relaxation modes related to networks strands and dangling chains as well as associative interaction between linear segments, in addition to vinylogous urethane bonds exchange.

The adhesive properties were studied in lap shear mode, showing best performance for PKHB 5% VU, including the possibility to thermally re-join the assembly after its mechanical failure. This is obtained thanks to the rapid relaxation times of this vitrimer, allowing strong adhesion to aluminum (typical of phenoxy resin), together with stiffness reinforcement typical of the crosslinked networks.

The preparation of PKHB 5% VU via melt reactive blending in a lab-scale micro extruder was also proved to yield consistent thermo-mechanical and rheological properties, thus demonstrating the production of phenoxy-based vinylogous urethane vitrimers in a solventless process, which opens for an industrially viable upscale of this class of materials, as a potential alternative to conventional epoxy thermosets.

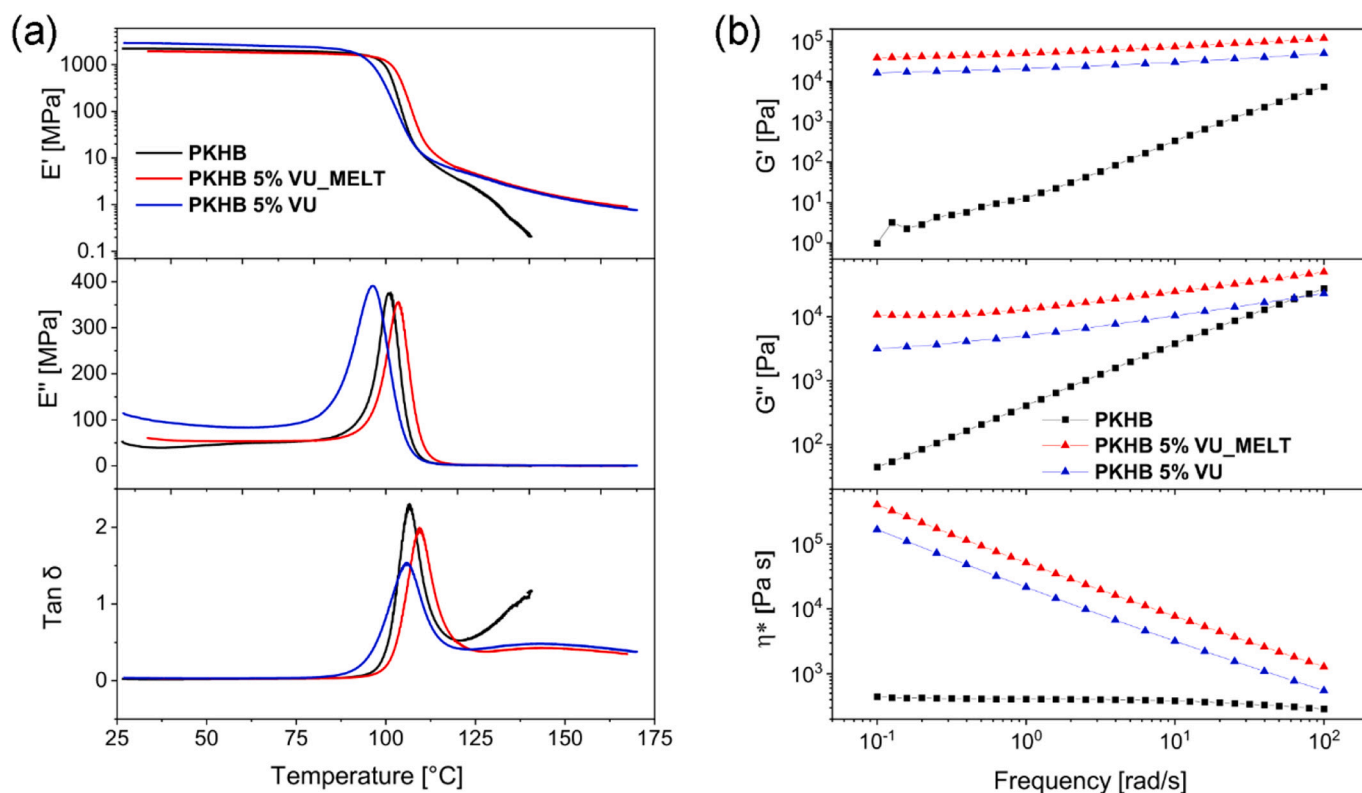


Fig. 7. Comparison between dynamo-mechanical (a) and rheological (b) properties for PKHB 5% VU prepared via the conventional solvent processing or by melt reactive processing.

CRedit authorship contribution statement

Giuseppe Soavi: Investigation, Visualization. **Francesca Portone:** Investigation, Visualization. **Daniele Battagazzore:** Investigation, Visualization. **Chiara Paravidino:** Investigation, Visualization. **Ros-sella Arrigo:** Formal analysis, Data curation. **Alessandro Pedrini:** Formal analysis, Data curation. **Roberta Pinalli:** Methodology, Validation, Funding acquisition. **Alberto Finà:** Conceptualization, Writing – original draft, Supervision, Funding acquisition. **Enrico Dalcanele:** Conceptualization, Writing – original draft, Supervision, Funding acquisition.

Declaration of Competing Interest

The authors declare no competing financial or personal interests.

Data availability

Data will be made available on request.

Acknowledgement

This work was supported by the Italian Ministry of University and Research under the PRIN 2017 projects 20179BJNA2 and by H2020-MSCA-RISE-2020 project VIT (N° 101008237). This work benefited from the equipment and framework of the COMP-HUB Initiative, funded by the “Departments of Excellence” program of the Italian Ministry for Education, University and Research (MIUR, 2018–2022). The authors acknowledge the Centro Interdipartimentale di Misure “G. Casnati” of the University of Parma for the use of NMR facilities.

Appendix A. Supplementary data

Supplementary data to this article can be found online at <https://doi.org/10.1016/j.reactfunctpolym.2023.105681>.

References

- [1] Closing the loop - An EU action plan for the Circular Economy. https://eur-lex.europa.eu/resource.html?uri=cellar:8a8ef5e8-99a0-11e5-b3b7-01aa75ed71a1.0012.02/DOC_1&format=PDF and, <https://ec.europa.eu/environment/circular-economy>.
- [2] D. Montarnal, M. Capelot, F. Tournilhac, L. Leibler, Silica-like malleable materials from permanent organic networks, *Science* 334 (2011) 965–968, <https://doi.org/10.1126/science.1212648>.
- [3] W. Denissen, J.M. Winne, F.E. Du Prez, Vitrimers: permanent organic networks with glass-like fluidity, *Chem. Sci.* 7 (2016) 30–38, <https://doi.org/10.1039/C5SC02223A>.
- [4] M. Capelot, D. Montarnal, F. Tournilhac, L. Leibler, Metal-catalyzed transesterification for healing and assembling of thermosets, *J. Am. Chem. Soc.* 134 (2012) 7664–7667, <https://doi.org/10.1021/ja302894k>.
- [5] A. Ruiz de Luzuriaga, R. Martin, N. Markaide, A. Rekondo, G. Cabañero, J. Rodríguez, I. Odriozola, Epoxy resin with exchangeable disulfide crosslinks to obtain reprocessable, repairable and recyclable fiber-reinforced thermoset composites, *Mater. Horiz.* 3 (2016) 241–247, <https://doi.org/10.1039/C6MH00029K>.
- [6] S. Zhao, M.M. Abu-Omar, Recyclable and malleable epoxy thermoset bearing aromatic imine bonds, *Macromolecules* 51 (2018) 9816–9824, <https://doi.org/10.1021/acs.macromol.8b01976>.
- [7] H. Memon, H. Liu, M.A. Rashid, L. Chen, Q. Jiang, L. Zhang, Y. Wei, W. Liu, Y. Qiu, Vanillin-based epoxy Vitriimer with high performance and closed-loop recyclability, *Macromolecules* 53 (2020) 621–630, <https://doi.org/10.1021/acs.macromol.9b02006>.
- [8] Y. Spiesschaert, M. Guerre, I. De Baere, W. Van Paeppegem, J.M. Winne, F.E. Du Prez, Dynamic curing agents for amine-hardened epoxy Vitrimers with short (Re) processing times, *Macromolecules* 53 (2020) 2485–2495, <https://doi.org/10.1021/acs.macromol.9b02526>.
- [9] T. Debsharma, V. Amfilochiou, A.A. Wróblewska, I. De Baere, W. Van Paeppegem, F. E. Du Prez, Fast dynamic siloxane exchange mechanism for reshapable vitriimer composites, *J. Am. Chem. Soc.* 144 (2022) 12280–12289, <https://doi.org/10.1021/jacs.2c03518>.

- [10] W. Denissen, G. Rivero, R. Nicolaj, L. Leibler, J.M. Winne, F.E. Du Prez, Vinylogous urethane vitrimers, *Adv. Funct. Mater.* 25 (2015) 2451–2457, <https://doi.org/10.1002/adfm.201404553>.
- [11] J. Tellers, R. Pinalli, M. Soliman, J. Vachon, E. Dalcanale, Reprocessable vinylogous urethane cross-linked polyethylene via reactive extrusion, *Polym. Chem.* 10 (2019) 5534–5542, <https://doi.org/10.1039/C9PY01194C>.
- [12] P. Haida, G. Signorato, V. Abetz, Blended vinylogous urethane/urea vitrimers derived from aromatic alcohols, *Polym. Chem.* 13 (2022) 946–958, <https://doi.org/10.1039/D1PY01237A>.
- [13] M. Capelot, M.M. Unterlass, F. Tournilhac, L. Leibler, Catalytic control of the Vitriimer glass transition, *ACS Macro Lett.* 1 (2012) 789–792.
- [14] S. Wu, Q. Chen, Advances and new opportunities in the rheology of physically and chemically reversible polymers, *Macromolecules* 55 (2022) 697–714, <https://doi.org/10.1021/acs.macromol.1c01605>, doi:10.1021/mz300239f.
- [15] L. Porath, J. Huang, N. Ramlawi, M. Derkaloustian, R.H. Ewoldt, C.M. Evans, Relaxation of Vitrimers with kinetically distinct mixed dynamic bonds, *Macromolecules* 55 (2022) 4450–4458, <https://doi.org/10.1021/acs.macromol.1c02613>.
- [16] A.M. Hubbard, Y. Ren, D. Konkolewicz, A. Sarvestani, C.R. Picu, G.S. Kedziora, A. Roy, V. Varshney, D. Nepal, Vitriimer transition temperature identification: coupling various thermomechanical methodologies, *ACS Appl. Polym. Mater.* 3 (2021) 1756–1766, <https://doi.org/10.1021/acsapm.0c01290>.
- [17] D.J. Fortman, J.P. Brutman, C.J. Cramer, M.A. Hillmyer, W.R. Dichtel, Mechanically activated, catalyst-free polyhydroxyurethane vitrimers, *J. Am. Chem. Soc.* 137 (2015) 14019–14022, <https://doi.org/10.1021/jacs.5b08084>.
- [18] Y. Spiesschaert, C. Taplan, L. Stricker, M. Guerre, J.M. Winne, F.E. Du Prez, Influence of the polymer matrix on the viscoelastic behaviour of vitrimers, *Polym. Chem.* 11 (2020) 5377–5385, <https://doi.org/10.1039/D0PY00114G>.
- [19] F. Snijkers, R. Pasquino, A. Maffezzoli, Curing and viscoelasticity of vitrimers, *Soft Matter* 13 (2017) 258–268, <https://doi.org/10.1039/C6SM00707D>.
- [20] J.P. Brutman, P.A. Delgado, M.A. Hillmyer, Polylactide Vitrimers, *ACS Macro Lett.* 3 (2014) 607–610, <https://doi.org/10.1021/mz500269w>.
- [21] Y. Nishimura, J. Chung, H. Muradyan, Z. Guan, Silyl ether as a robust and thermally stable dynamic covalent motif for malleable polymer design, *J. Am. Chem. Soc.* 139 (2017) 14881–14884, <https://doi.org/10.1021/jacs.7b08826>.
- [23] M. Röttger, T. Domenech, R. van der Weegen, A. Breuillac, R. Nicolaj, L. Leibler, High-performance vitrimers from commodity thermoplastics through dioxaborolane metathesis, *Science* 356 (2017) 62–65, <https://doi.org/10.1126/science.aah528>.